Journal of Petroleum Science and Engineering 71 (2010) 138–146

Contents lists available at ScienceDirect

Journal of Petroleum Science and Engineering

journal homepage: www.elsevier.com/locate/petrol

Research paper

A fully-coupled thermal multiphase wellbore flow model for use in reservoir simulation

S. Livescu [a,*], L.J. Durlofsky [a], K. Aziz [a], J.C. Ginestra [b]

[a] Department of Energy Resources Engineering, Stanford University, Stanford, CA 94305, USA
[b] Shell Oil Company, Two Shell Plaza, Houston, TX 77002, USA

ARTICLE INFO

Article history:
Received 16 September 2008
Accepted 20 November 2009

Keywords:
black-oil model
drift-flux model
multiphase flow
multisegment well
nonisothermal flow
wellbore flow

ABSTRACT

A numerical thermal multiphase wellbore flow model is developed and applied. The formulation entails one-dimensional spatial (axial) and temporal discretizations and includes coupled mass conservation equations for oil, water and gas components, three-phase fluid flow, an energy conservation equation, and a pressure drop relationship. A drift-flux model is employed to represent slip between fluid phases. The model is implemented into a reservoir simulator to enable fully coupled reservoir-wellbore simulations. A series of numerical results are presented, including validation against previous experimental results, verification against an analytical model, and simulations of complex thermal multiphase flow scenarios that involve vertical and multilateral wells coupled with oil reservoir models. Taken in total, these numerical simulation results demonstrate the broad applicability and robustness of the new wellbore flow model.

1. Introduction

There are vast resources of heavy oil, tar sands and oil shales, much of which is in the United States and Canada, that cannot be efficiently produced using conventional oil recovery techniques (U.S. Department of Energy, 2004, 2007). Rather, the production of these resources requires the introduction of substantial quantities of heat into the subsurface formation. In the case of heavy oil and tar sands, steam injection is applied to increase formation temperatures to around 100–150 °C and thus decrease the oil viscosity, enabling flow (and production) at reasonable pressure gradients. In the case of oil shales, one of the proposed production schemes, currently in the pilot stage, entails the use of downhole electrical heaters to heat the formation to very high temperatures (about 340–370 °C) over a period of approximately four years. At these temperatures, oil shale, which contains up to 15% hydrocarbon by weight and is an oil precursor, converts to what is essentially a light crude oil. Liquid hydrocarbons are then recovered using vertical wells.

The design, management and optimization of all of the processes noted above require accurate models for thermal multiphase flow in wellbores. This modeling is very challenging due to the complex interplay of a variety of physical phenomena. Practical models are generally numerical, with some of the underlying representations specified through empirical relationships. For applications in oil recovery, wellbore flow models must be linked to reservoir simulators. This linkage introduces additional complications.

Over the past few decades, many studies geared toward the modeling of thermal multiphase flow in pipes and wellbores have been presented in the literature. These include both analytical and numerical models. The first analytical model was presented by Ramey (1962). Under the assumption of single-phase flow, his model provides the temperature inside the well as a function of depth and time. Hasan and Kabir (2002); Hasan et al. (2005) (see also references therein) further generalized these models by including two-phase flow, kinetic energy and Joule-Thompson effects. In a recent paper (Livescu et al., 2008b), we also proposed analytical models that are valid for multiphase flows in advanced (e.g., multilateral) wells. Other researchers, e.g., Izgec et al. (2007), have extended these wellbore models to include approximate (single-phase radial flow) treatments for influx from the reservoir.

Several fully-coupled numerical models for thermal wellbore flow have been presented (e.g., Stone et al., 1989, 2002; Pourafshary et al., 2009) within the context of general purpose reservoir simulation. These formulations are more general than the models discussed above. Specifically, the fully-coupled numerical models involve one-dimensional (axial) representations of the wellbore and include coupled conservation equations for multiple components (e.g., oil, water and gas), an energy equation, and a pressure drop relationship. Flow from the reservoir into the wellbore (in the case of a production well) provides source terms for the wellbore flow model. Previous formulations have been developed for both black-oil models (Stone et al., 1989, 2002), in which the system is represented in terms of oil and gas 'pseudocomponents' and water, and fully compositional

* Corresponding author.
E-mail address: slivescu@stanford.edu (S. Livescu).

0920-4105/$ – see front matter © 2009 Published by Elsevier B.V.
doi:10.1016/j.petrol.2009.11.022

models (Stone et al., 2002; Pourafshary et al., 2009), in which the system contains an arbitrary number of components (e.g., methane, ethane), pseudocomponents and water.

The models introduced by Stone et al. (1989, 2002) simulate the hydrodynamics and thermal effects in both the wellbore and the reservoir. This capability is achieved by discretizing the well into segments and solving the well equations implicitly with the reservoir equations. The first model of Stone et al. (1989) is a three-component, three-phase black-oil model in which the flow regime is classified as stratified, bubbly, slug or mist, based on experimental data. The second model (Stone et al., 2002), which has been implemented into a commercial software package, treats isothermal compositional systems and isothermal and thermal black-oil systems. A drift-flux model is used to represent the flow inside the well in the isothermal models. For thermal simulations, a homogeneous (without slip) model is used. The recent work of Pourafshary et al. (2009) extends these models. Specifically, these authors developed a thermal compositional formulation which they implemented into a coupled reservoir/wellbore simulator. This model accounts for slip between the gas and liquid phases. Their approach is simpler than a full three-phase drift-flux treatment, as they assume no slip between liquid phases.

The fully-coupled numerical model for thermal wellbore flow presented in this paper has a number of important features that distinguish it from previous developments. In contrast to the models of Stone et al., we incorporate a drift-flux representation, which enables us to capture slip between phases including complex physical phenomena such as counter-current flow.

In contrast to the formulation of Pourafshary et al., our wellbore model includes a thermal drift-flux representation and accumulation terms (time derivatives) in both the mass and energy conservation equations. These terms can be important when the flow is not steady state. Our applications, which include multilateral wells, are more complex than those considered previously.

As indicated above, in our formulation we employ a drift-flux model to represent multiphase flow in the wellbore (or pipe). Models of this type have been used for some time in thermal-hydraulic analysis codes, especially in the nuclear industry (see for example (Ishii and Mishima, 1984; Masella et al., 1998; Bonizzi and Issa, 2003; Hibiki and Ishii, 2003; Issa and Kempf, 2003; Ishii and Hibiki, 2006; Hoeld, 2007). They have also been used extensively in oil reservoir simulation applications (see, e.g., Holmes et al., 1998; Shi et al., 2005, 2005). Drift-flux models are well-suited for coupling with the reservoir flow equations because they are relatively simple, continuous and differentiable.

Practical drift-flux models have a significant empirical component and thus require a number of experimentally determined parameters (another option is to apply a mechanistic model to determine these parameters, but even mechanistic models require empirical parameters for closure). Oddie et al. (2003) performed an extensive experimental study of two and three-phase flows in 15 cm diameter inclined pipes. Gas–water, oil–water, and gas–oil–water systems were considered. Based on these experimental data, Shi et al. (2005) developed a unified drift-flux model for two and three-phase flows. For three-phase systems, this model accounts for the effect of the gas phase on the volume fractions of the two liquid phases (as a function of inclination angle). This model is now used in several simulators and will be applied here to relate phase fractions and velocities to the total (mixture) velocity. The liquid-liquid slip has been largely ignored in the literature because of the difficulty of modeling this phenomenon and because of the lack of experimental data. However, the slip between the two liquid phases can be substantial, especially for low-rate inclined wells. For example, Oddie et al. (2003) observed significant slip between oil and water phases for a pipe inclination of 45° at a total liquid rate of 20 m^3/h in a 15 cm diameter pipe.

In a companion paper (Livescu et al., 2008b), we developed and tested a semianalytical procedure that entails the use of analytical solutions for wellbore temperature coupled sequentially with numerical solutions of the wellbore mass conservation and pressure drop equations. The wellbore mass conservation and pressure drop equations were solved together with the reservoir equations. The formulation presented here represents the basis for this semianalytical procedure and provides benchmark results against which the semianalytical computations can be compared.

This paper proceeds as follows. We first present the equations describing thermal multiphase flow in pipes and wellbores. The drift-flux model is also briefly described. We then present our numerical discretization and discuss the linkage of the wellbore model with the reservoir simulator, which in this case is Stanford's General Purpose Research Simulator (GPRS), described in (Cao, 2002; Jiang, 2007). A series of numerical results is then presented. These include a validation of the numerical model through comparison to the experimental data of Hasan and Kabir (2002), verification of the model through comparison to analytical results, numerical results for a multilateral well with three-phase flow and inflow (production) at many locations along the well, and a two-phase (gas–water) flow problem with phase change (vaporization). Finally, conclusions and recommendations for further work are presented.

2. Model formulation

In this section we present the equations governing wellbore flow with thermal effects. The models are one-dimensional, with variables resolved in the axial direction only. We consider a system with three components, referred to as oil, water, and gas (by definition components are phases at some reference pressure and temperature, usually standard conditions) and three fluid phases, also referred to as oil, water, and gas. We apply the black-oil formulation, which is commonly used in reservoir flow simulation.

The governing equations include mass balance equations for each component along with an energy balance equation and a momentum balance equation. The unknowns are the in situ gas and water phase volume fractions, designated α_g and α_w, wellbore pressure, p^w, mixture velocity (total volumetric flow rate divided by pipe area), V_m, and wellbore temperature, T^w. The oil phase volume fraction, α_o, can be computed from the relationship $\alpha_o = 1 - \alpha_g - \alpha_w$. The local volume fraction of phase p (p = oil, water, gas) is defined as $\alpha_p = A_p/A^w$, i.e., the ratio between the area occupied by the phase, A_p, and the total cross-sectional pipe area, A^w. The well is discretized spatially into a number of segments, and the unknowns listed above are determined for each segment as functions of time and position.

2.1. Drift-flux model for phase velocities in well

We apply a drift-flux model to represent the superficial velocities V_{sp} appearing in the conservation equations. This model was originally introduced by Zuber and Findlay (1965) for two-phase flows. It is particularly well suited for use in a reservoir simulator as it is relatively simple, continuous and differentiable.

For a gas–liquid flow in a vertical pipe, Zuber and Findlay expressed the gas velocity (averaged across the pipe area) as a sum of two terms, as shown in Fig. 1,

$$V_g = C_0 V_m + V_d \tag{1}$$

where C_0 is a profile parameter (also referred to as a distribution coefficient) and V_d is the drift velocity of gas relative to the liquid. For this particular configuration, the gas inside the pipe moves faster than the liquid as a result of two mechanisms, specifically the higher concentration of gas near the center of the pipe, where velocity is higher (this effect is captured by the term $C_0 V_m$ in Eq. (1)) and the tendency of the gas to rise in the pipe due to buoyancy (V_d). The

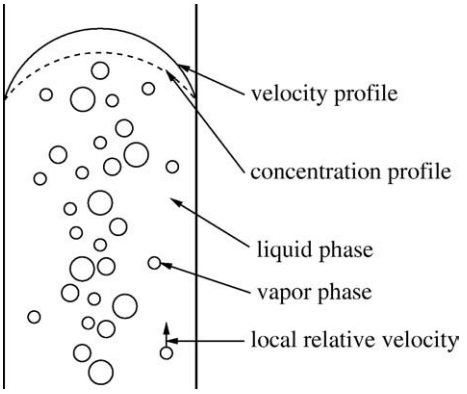

Fig. 1. Schematic depiction of the drift-flux model illustrating slip between phases.

average mixture velocity is the sum of the gas and liquid superficial velocities,

$$V_m = V_{sg} + V_{sl} = \alpha_g V_g + (1-\alpha_g)V_l. \tag{2}$$

Our implementation of the drift-flux model, particularly the functional forms for C_0 and V_d (which depend on α_p, V_m and θ), follows the work of Shi et al. (2005, 2005). These model parameters were determined from an extensive set of large-scale pipe flow experiments performed by Oddie et al. (2003) for one, two and three-phase flows at various inclinations θ. The drift-flux parameters were determined through an optimization procedure which minimized the square differences between experimental results and model predictions. The resulting models are applicable for gas–liquid, oil–water, and gas–oil–water flows at various θ. We note that the model parameters can be readily tuned for particular two or three-phase flow systems if data are available.

In the particular case in which all phases have the same velocity, $V_p = V_m$, the drift-flux model reduces to the homogeneous model. In this case, $C_0 = 1$ and $V_d = 0$. The homogeneous model was also implemented in this work, allowing direct comparison with the drift-flux model.

The incorporation of temperature effects in the drift-flux model described above adds an additional degree of complexity. In our extension of this model to the thermal case, we include the temperature dependence of density, which in turn affects the phase velocities in the drift-flux model.

2.2. Pressure drop equation

Within the context of drift-flux modeling, two basic approaches have been described in the literature for computing the pressure profile along the well or pipe. More rigorous procedures, e.g., (Hibiki and Ishii, 2003; Issa and Kempf, 2003), apply a general conservation of momentum equation. Simpler approaches, used within the context of oil reservoir simulation, involve the use of a so-called pressure drop equation. Here we will briefly discuss the more general momentum balance approach and then describe the pressure drop equation used in this work. Correspondences between the two approaches will be noted.

Consider the case of two-phase (gas–liquid) flow. By summing the momentum conservation equations for the individual phases and then area averaging, a one-dimensional momentum balance equation for the entire fluid can be obtained. Assuming the coordinate z points along the well, this equation is given by Hibiki and Ishii (2003); Issa and Kempf (2003) as:

$$\frac{\partial p^w}{\partial z} = -\rho_m \overline{g} - \frac{\partial}{\partial t}(\rho_m V_m) - \frac{\partial}{\partial z}(\rho_m V_m^2) - \frac{f_{tp}\rho_m V_m |V_m|}{2d_{in}} - R. \tag{3}$$

Here, ρ_m is the mixture density given by $\rho_m = \alpha_g\rho_g + \alpha_l\rho_l$, with ρ_g and ρ_l the phase densities (subscript l represents liquid). The parameter $\overline{g}$ is the z component of gravitational acceleration and d_{in} is the internal diameter of the well. The last term in Eq. (3) is due to the slip between the two phases and can be written (using our notation) as

$$R = \frac{\partial}{\partial t}(\alpha_g\rho_l V_d) + \frac{\partial}{\partial z}\left[2\alpha_g\rho_l V_m V_d - \alpha_g((1-\alpha_g)\rho_g + \alpha_g\rho_l)V_d^2\right]. \tag{4}$$

The frictional force per unit volume between the overall fluid and the wall is evaluated through the friction factor f_{tp}, which depends on a number of parameters, including the pipe roughness. Comprehensive discussions regarding f_{tp} appear in the literature (Govier and Aziz, 1972; Ishii and Mishima, 1984; Hibiki and Ishii, 2003; Issa and Kempf, 2003; Ishii and Hibiki, 2006). In general, f_{tp} is dependent on the flow regime and is obtained from experimental data.

The approach based on the pressure drop equation (Govier and Aziz, 1972; Stanislav et al., 1986; Hasan and Kabir, 2002) represents the total pressure loss over any segment of the well as the sum of three components:

$$\Delta p^w = \Delta p_h^w + \Delta p_a^w + \Delta p_f^w \tag{5}$$

where Δp_h^w is the hydrostatic pressure loss, Δp_a^w is the pressure loss due to acceleration, or kinetic energy change, and Δp_f^w is the pressure loss due to frictional effects. These terms are given by (e.g., Govier and Aziz, 1972):

$$\Delta p_h^w = -\rho_m \overline{g} \tag{6}$$

$$\Delta p_a^w = -\frac{\partial}{\partial t}(\rho_m V_m) - \frac{\partial}{\partial z}(\rho_m V_m^2) \tag{7}$$

$$\Delta p_f^w = -\frac{f_{tp}\rho_m V_m |V_m|}{2d_{in}}. \tag{8}$$

In typical reservoir simulation problems, the pressure loss due to acceleration is small compared with the gravitational and frictional pressure losses.

Comparing Eq. (5) with the momentum balance Eq. (3), it is apparent that the difference between the two representations is that the pressure drop equation does not include the $\mathcal{R}$ term. This term is of a similar form as the accelerational pressure loss Eq. (7). It is therefore reasonable to expect that the $\mathcal{R}$ term will be small relative to Δp_h^w and Δp_f^w in many practical cases. It is possible, however, that this term is important for some flow regimes, as it involves both V_m and V_d. Therefore, we believe that further analysis is warranted and, if necessary, treatments for computing $\mathcal{R}$ within the context of coupled wellbore flow modeling should be developed. We note finally that additional terms appear in the case of three-phase flow (Bonizzi and Issa, (2003)), and these too should be evaluated and modeled as required.

There is an additional complication that arises in wellbore flow modeling that does not appear in other application areas, namely the impact of inflow through the perforations on f_{tp}. Ouyang and Aziz (2002) investigated this effect and showed that f_{tp} should be modified based on the inflow or outflow Reynolds number. This effect should therefore also be included in both the momentum balance and pressure drop models.

2.3. Mass conservation equations

The mass conservation equations for the gas, oil and water components are, respectively,

$$\frac{\partial}{\partial t}(\rho_g\alpha_g\chi_{gg} + \rho_o\alpha_o\chi_{go} + \rho_w\alpha_w\chi_{gw}) + \frac{\partial}{\partial z}(\rho_g V_{sg}\chi_{gg} + \rho_o V_{so}\chi_{go} + \rho_w V_{sw}\chi_{gw}) = m_{gg} + m_{go} + m_{gw} \tag{9}$$

$$\frac{\partial}{\partial t}(\rho_o\alpha_o\chi_{oo} + \rho_g\alpha_g\chi_{og}) + \frac{\partial}{\partial z}(\rho_o V_{so}\chi_{oo} + \rho_g V_{sg}\chi_{og}) = m_{oo} + m_{og} \tag{10}$$

$$\frac{\partial}{\partial t}(\rho_w\alpha_w\chi_{ww}) + \frac{\partial}{\partial z}(\rho_w V_{sw}\chi_{ww}) = m_{ww}. \tag{11}$$

Here, ρ_p and α_p represent the density and the in situ volume fraction of phase p (p = water, oil, gas), respectively, χ_{cp} is the molar fraction of component c (c = water, oil, gas) in phase p, V_{sp} is the superficial velocity of phase p and m_{cp} is the source/sink term at each segment along the well (we use p to designate both pressure and phase, though the meaning should be clear from the context). Note that, as indicated above, the gas component can reside in all three phases, the oil component in the oil and gas phases, and the water component only in the water phase. Thus, the general model can handle volatile oils, as the oil component can exist in the gas phase. Eqs. (9)–(11) can be readily generalized to the case when all components exist in all phases.

The time derivative terms in the mass balance equations represent the mass accumulation of the components, while the spatial derivative terms represent the convective flux of the components.

Again, the superficial velocity of phase p is defined as the product of the phase velocity and the local phase fraction, $V_{sp} = \alpha_p V_p$. The mixture velocity can be expressed as $V_m = V_{sg} + V_{so} + V_{sw}$.

In writing the generalized black-oil equations above, we assume instantaneous local thermodynamic equilibrium in the reservoir and the wellbore. Thus, the pressure–volume–temperature (PVT) properties can be related to phase properties. Specifically, the equilibrium ratios (K-values, which are prescribed as input) relate the mass fraction of component c in phase p_1 to the mass fraction of the same component in phase p_2 as functions of pressure and temperature. For example, K_g^{og} relates the mole fraction of the gas component in the oil phase to that in the gas phase:

$$K_g^{og}(p,T) = \frac{\chi_{go}}{\chi_{gg}}. \tag{12}$$

All other required relationships between the PVT and phase properties are well documented in the literature (Aziz and Wong, 1988, 1989; Farouq Ali and Abou-Kassem, 1988, 1989; Aziz and Settari, 2002). Standard black-oil properties (solubility ratios and formation volume factors) can be related to equilibrium ratios. The relationships given above are for isothermal models. For thermal systems, additional correlations are needed to account for temperature effects. For example, here the temperature variation of the density of phase p is evaluated as

$$\rho_p(p,T) = \frac{\rho_p^T(p_{ref},T)\rho_p^p(p,T_{ref})}{\rho_{p,ref}(p_{ref},T_{ref})} \tag{13}$$

where p_{ref} and T_{ref} are the reference pressure and temperature, respectively. Other representations are also possible (Aziz and Wong, 1988, 1989; Farouq Ali and Abou-Kassem, 1988, 1989).

In some cases, such as in pipeline simulations, source/sink terms can be specified directly (e.g., $m_{oo}(z,t)$ is prescribed). However, in the case of oil reservoir simulation, source/sink terms involve coupling between the well and the reservoir. In this case the source/sink term depends on the well and reservoir pressures, in addition to other reservoir data. Specifically, for a production well, the source term can be written as

$$m_{cp} = \rho_p q_{cp}^w = W\lambda_p\rho_p\chi_{cp}(p_p - p^w) \tag{14}$$

where q_{cp}^w is the volumetric flow of component c in phase p from the reservoir into the well, λ_p is the phase mobility, which depends on reservoir pressure and fluid saturations, and W is the well index, which depends on the reservoir simulation grid, reservoir properties and well diameter, and p_p is the phase pressure in the grid block in which the particular well segment is located. The well index W can be computed using standard procedures (Peaceman, 1977).

2.4. Energy conservation equation

The energy conservation equation for the overall fluid can be written in a variety of forms (Ramey, 1962; Satter, 1965; Ishii and Mishima, 1984; Farouq Ali and Abou-Kassem, 1988, 1989; Sharma et al., 1989; Holmes et al., 1998; Hasan and Kabir, 2002; Stone et al., 2002; Hibiki and Ishii, 2003; Cheng and Mewes, 2006; Ishii and Hibiki, 2006). We express it as follows:

$$\frac{\partial}{\partial t}\sum_p \rho_p\alpha_p\left(u_p + \frac{1}{2}V_p^2\right) = -\frac{\partial}{\partial z}\sum_p \rho_p V_{sp}\left(h_p + \frac{1}{2}V_p^2\right) + \sum_p \rho_p V_{sp}\,\overline{g} - Q_{loss} + m_h \tag{15}$$

where u_p and h_p are the specific internal energy and the enthalpy of phase p, respectively. The time derivative term represents the energy accumulation and the spatial derivative term represents the flux of energy due to convection and work done by pressure forces. The other two terms represent the rate of work done on the fluid by gravitational forces and heat losses to the surroundings. We ignore conductive heat transfer in the axial direction. The source term in Eq. (15) is similar to those in the mass conservation equations, the molar fractions being replaced by specific enthalpies,

$$m_h = \sum_p W\lambda_p\rho_p h_p(p_p - p^w) \tag{16}$$

The specific internal energy and enthalpy of phase p are

$$u_p = (c_p)_p(T^w - T_{ref}) \tag{17}$$

$$h_p = u_p + \frac{p^w}{\rho_p} \tag{18}$$

where $(c_p)_p$ represents the specific heat of phase p, which is defined at the reference temperature T_{ref}. Phase change terms do not appear in Eq. (15) because we write the energy equation for the entire fluid system rather than for each phase individually, and thus the phase change terms cancel. We note also that the Joule-Thompson effect is included in the formulation through our general treatment of h_p. For example, through the representation of $\rho_p(p^w, T^w)$ in Eq. (18), the Joule-Thompson coefficient μ_{JT} for the gas phase is given by

$$(\mu_{JT})_g = -\frac{1}{(c_p)_g}\left\{\frac{1}{\rho_g} - T\left[\frac{\partial}{\partial T}\left(\frac{1}{\rho_g}\right)\right]_p\right\} \tag{19}$$

This quantity is nonzero.

In Eq. (15), the heat loss term Q_{loss} must be approximated, and many models have been proposed. Here we assume that the heat loss to the surroundings can be represented in terms of an overall heat transfer coefficient, U_{to}, which can be written as a sum of thermal

resistances. In our case these resistances are those of the tubing, annulus fluid, casing and cement. The heat loss to the surroundings is then given by

$$Q_{loss} = -2\pi r_{in} U_{to}(T - T^w) \tag{20}$$

where $r_{in} = d_{in}/2$ is the internal radius of the well and T is the temperature external to the wellbore, which in our case is the reservoir temperature. For a detailed discussion of the determination of the overall heat transfer coefficient, see Prats (1982). In this work, the overall heat transfer coefficient does not vary in time, although time-dependent overall heat transfer coefficients could be easily treated. Models with time-dependent overall heat transfer coefficients have been presented previously by Ramey (1962), Hasan and Kabir (2002), Izgec et al. (2007).

We note finally that, in the case of water-steam phase change, an extra constraint is needed in addition to the energy equation. When only one phase exists (gas or water), the temperature and pressure are independent, while in the two-phase region, the temperature is dependent on the saturation pressure,

$$p^w = p^w_{sat}(T^w). \tag{21}$$

Both the saturation pressure and the temperature in the two-phase region are interpolated from steam tables (Keenan et al., 1969). This constraint was also used in previous well models (see for example (Stone et al., 1989)).

Prior to describing the numerical implementation, we review some of the inherent assumptions and limitations of our thermal multiphase wellbore flow model. These are as follows:

- In the current model, the fluids are always represented as black-oils with constant bubble point. Extension to compositional systems requires an expanded set of equations and a full treatment of phase behavior. In recent work (Livescu et al., 2009), we developed a prototype formulation for compositional systems.
- The current model allows exchange between the oil and gas phases. When oil and gas components are present, the water component can reside only in the water phase. The maximum number of components that the model can treat is three.
- In the case of a water-steam system in which no hydrocarbon components are present, the water component can reside in both the gas and liquid phases. We show an example of such a case in the results below.
- The wellbore model is transient and one-dimensional, with variables resolved in the axial direction. A drift-flux representation is used to model slip between phases within the wellbore. This model requires a number of empirical coefficients.

3. Numerical implementation

The well equations presented above are solved fully-coupled (implicitly) with the reservoir flow equations. As explained earlier, the reservoir model provides the source terms (and/or boundary conditions) for the wellbore model. For a three-phase, three-component system, the reservoir model consists of three mass conservation equations and an energy conservation equation, along with capillary pressure relationships and a saturation constraint. The variables associated with the reservoir are the phase pressures, gas and oil saturations (in situ phase fractions), and temperature. These equations are discretized using a finite volume procedure. Detailed descriptions of the simulation procedure are given by Aziz and Wong (1988, 1989) and Farouq Ali and Abou-Kassem (1988, 1989).

The well is discretized into N_s segments. All variables are taken to be constant within a segment. As indicated in Fig. 2, for segment i, the mixture velocity is defined at the upper (exit) boundary of the cell, the pressure and temperature are defined at the lower boundary, and the gas and water phase volume fractions at the center of the cell. These quantities are defined at different locations within the segment to more easily incorporate boundary conditions and to facilitate linkage with the reservoir simulator. The system of equations, corresponding to the mass and energy conservation equations for the well and reservoir, is linearized using Newton's method. The linear system is written as $\mathbf{J}\delta = -\mathbf{R}$, where $\mathbf{J}$ is the Jacobian matrix, δ is the update vector and $\mathbf{R}$ is the residual vector.

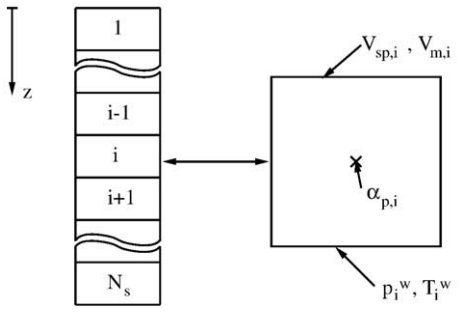

Fig. 2. Schematic representation of the discretized wellbore and the locations at which the different variables are defined.

The discretized forms of the well equations, which provide the residual equations for the well, are given by:

$$R^w_{p,i} = (p^w_i - p^w_{i-1}) - \Delta p^w_{h,i} - \Delta p^w_{f,i} - \Delta p^w_{a,i} = 0 \tag{22}$$

$$\begin{aligned} R^w_{c,i} = {} & \frac{\Delta z}{\Delta t} A_i \left[\left(\sum_p \rho_p \alpha_p \chi_{cp} \right)^{n+1}_i - \left(\sum_p \rho_p \alpha_p \chi_{cp} \right)^{n}_i \right] \\ & - A_i \left[\left(\sum_p \rho_p V_{sp} \chi_{cp} \right)^{n+1}_{i+1} - \left(\sum_p \rho_p V_{sp} \chi_{cp} \right)^{n+1}_i \right] \\ & - \left[W \sum_p \lambda_p \rho_p \chi_{cp} (p_p - p^w) \right]^{n+1}_i = 0 (c = g, o, w;\ p = g, o, w) \end{aligned} \tag{23}$$

$$\begin{aligned} R^w_{e,i} = {} & \frac{\Delta z}{\Delta t} A_i \left\{ \left[\sum_p \rho_p \alpha_p \left(u_p + \frac{1}{2} V_p^2 \right) \right]^{n+1}_i - \left[\sum_p \rho_p \alpha_p \left(u_p + \frac{1}{2} V_p^2 \right) \right]^{n}_i \right\} \\ & - A_i \left\{ \left[\sum_p \rho_p V_{sp} \left(h_p + \frac{1}{2} V_p^2 \right) \right]^{n+1}_{i+1} - \left[\sum_p \rho_p V_{sp} \left(h_p + \frac{1}{2} V_p^2 \right) \right]^{n+1}_i \right\} \\ & - V_i \left(\sum_p \rho_p V_{sp}\ \overline{g} \right)^{n+1}_i + \Delta z (Q_{loss})^{n+1}_i - (m_h)^{n+1}_i = 0 \end{aligned} \tag{24}$$

where i and $i+1$ designate segments, n and $n+1$ designate time levels, A_i and V_i are the cross-sectional area and the volume of segment i, Δz and Δt are the segment lengths and time steps, respectively, and $\overline{g} = g \cos\theta$. Note that, in Eq.(23), $\chi_{wo} = \chi_{wg} = \chi_{ow} = 0$. The pressure drop equation is used for all segments except the first one. For this segment a constraint equation is applied, which can specify either the rate of any phase (other specifications such as total rate are also possible) or a bottom hole pressure (BHP). Similar (three-dimensional) discretizations provide residual equations for the reservoir domain.

We use the standard Godunov first order implicit upwinding scheme for discretizing the mass and energy conservation Eqs. (23) and (24). The discretizations as written are for a production well for which the V_{sp} are all negative (positive z points downwards). The upwinding of the convection terms is switched when any of the V_{sp} are positive. In the case of counter-current flow, different phases may flow in different directions, so the upwind direction must be evaluated for each phase individually. The scheme is implicit, as all quantities outside of the accumulation term are evaluated at time $n+1$.

The Jacobian matrix **J** has four parts, designated $\mathbf{J}_{RR}$, $\mathbf{J}_{RW}$, $\mathbf{J}_{WR}$ and $\mathbf{J}_{WW}$. The first subscript indicates the domain (*R* for reservoir, *W* for well) from which the residual equation derives and the second subscript indicates if the derivative is with respect to a reservoir or well variable. A schematic representation of **J** is shown in Fig. 3. The Jacobian is built such that the energy equations and the temperature unknowns (for both the reservoir and well domains) appear at the end of their respective sets. For isothermal problems these equations and unknowns are dropped and the Jacobian is otherwise the same.

4. Numerical results

We now apply our numerical model to investigate several different cases involving thermal flow in wellbores. In all cases, Stanford's General Purpose Research Simulator (GPRS) is used. By specifying a very simple reservoir model to provide the source terms for the well in the validation and verification examples, the coupled reservoir-wellbore simulator to some extent emulates a standalone wellbore simulator. Additional applications are presented in (Livescu et al., 2008a).

4.1. Validation using experimental data

The first example provides a validation of our numerical model against experimental data (Hasan and Kabir, 2002). Consistent with the experimental set up, we have a vertical well of length 1632 m (5355 ft) and interior diameter $d_{in}=0.0762$ m (3 in) with one perforation at its bottom (at $z=L$). The wellbore pressure at segment 1 (top of the well), p_1^w, is 779.1 kPa (113 psi). The fluid flow rates at standard conditions are $q_o=9.380$ m^3/day (59 STB/day), $q_w=86.17$ m^3/day (542 STB/day) and $q_g=1161$ m^3/day (41 Mcf/day). These rates are achieved in the simulations through appropriate specification of the phase saturations in the reservoir and the parameters appearing in Eq. (14). Phase densities at standard conditions are $\rho_o=853.4$ kg/m^3, $\rho_w=1010$ kg/m^3 and $\rho_g=1.32$ kg/m^3.

The surrounding temperature is defined by a geothermal gradient, increasing from 24.44 °C (76 °F) at the top of the well to 42.22 °C (108 °F) at the bottom of the well. Hasan and Kabir (2002) used a depth-dependent overall heat transfer coefficient in their model for this problem. We apply their values in our solution (i.e., U_{to} is not a matching parameter). The drift-flux model is used for this calculation and the well is kept under BHP control. The reservoir model is specified such that an essentially steady-state wellbore flow is achieved.

The comparison between our numerical results, labeled 'GPRS,' and the experimental data, labeled 'measured,' is shown in Fig. 4, together with the geothermal reservoir temperature. The agreement is clearly very close between the simulation results and the experimental data. These results, although for a simple system, provide a degree of validation for our thermal wellbore flow model.

4.2. Verification against analytical solution

We compared numerical results using the fully-coupled model to analytical solutions for a number of cases, both steady-state and transient, and achieved very close agreement for temperature along the wellbore (this is the quantity provided by the analytical solutions) in all cases. The next example, which involves steady-state three-phase flow, is representative. The well is vertical (1524 m in length, 0.0762 m interior diameter) and is open to the reservoir only at $z=L$. We specify $p_1^w=779.1$ kPa. The fluid flow rates at standard conditions are $q_o=321.1$ m^3/day, $q_w=80.77$ m^3/day and $q_g=1903$ m^3/day. Steady-state conditions with these rates are achieved through appropriate specification of the reservoir parameters as in the first example. The overall heat-transfer coefficient is $U_{to}=105.2$ W/(m^2 °C). The drift-flux model is employed. The analytical solution for this case is expressed in terms of an integral which can be evaluated easily (see Livescu et al., 2008b for the specific expression).

Results for the temperature along the wellbore for this case are shown in Fig. 5. There is clearly very close agreement between the numerical and analytical models. An additional comparison between the numerical and analytical solution for a transient example is given in (Livescu et al., 2008b), where a similar level of agreement is achieved. This very close correspondence between the numerical and analytical solutions is reassuring and can be viewed as a verification of our numerical implementation of the thermal wellbore flow model.

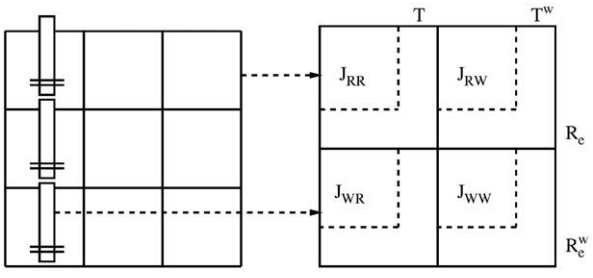

Fig. 3. Schematic representation of the full Jacobian matrix.

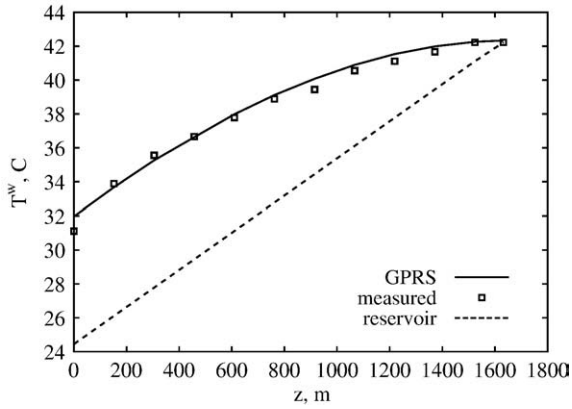

Fig. 4. Validation of the numerical results against experimental data reported by Hasan and Kabir (2002). 'GPRS' indicates the numerical result, 'measured' indicates the experimental data, and 'reservoir' depicts the surrounding temperature (which varies due to the geothermal gradient). The overall heat transfer coefficient is depth-dependent.

4.3. Numerical results for complex cases

We now demonstrate the performance of the numerical model for more general scenarios. We first consider a multilateral well with three

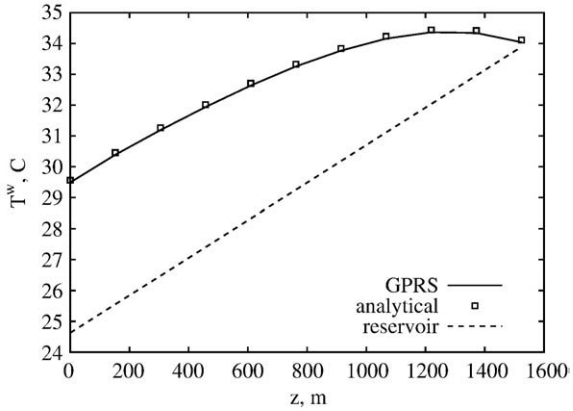

Fig. 5. Verification of the numerical results against an analytical solution for the three-phase case. The drift-flux model is used. 'GPRS' and 'analytical' represent the numerical and analytical results. Surrounding temperature varies due to geothermal gradient.

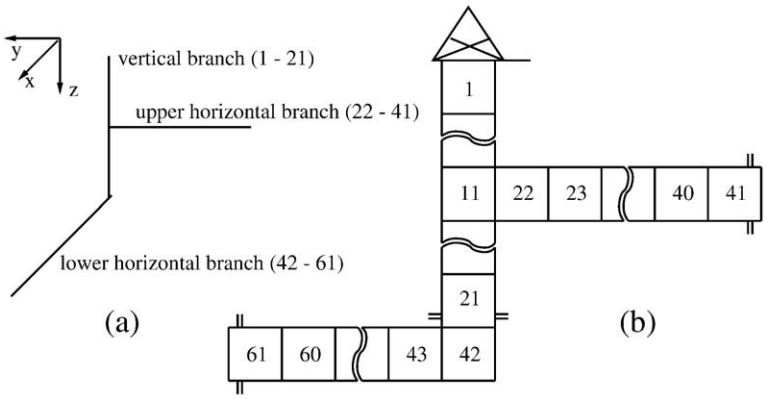

Fig. 6. Schematic representation of multilateral well: (a) orientation of the well in 3D, and (b) segment numbering.

different branches. A schematic of this model is shown in Fig. 6. Note that the two horizontal branches are in different planes. Each branch is 304.8 m (1000 ft) long, of interior diameter 0.0762 m (3 in.), and is open to the reservoir only at its end (as depicted in Fig. 6). The vertical branch has segments numbered from 1 to 21 (segment 21 is perforated), the upper horizontal branch contains segments 22 to 41 (segment 41 is perforated) and the lower horizontal branch contains segments 42 to 61 (segment 61 is perforated). Segment 22 of the upper horizontal branch is connected to segment 11 of the vertical branch and segment 42 of the lower horizontal branch is connected to segment 21 of the vertical branch. The well is operated under BHP control with $p_1^w = 30.23$ MPa (4400 psia). The system contains three phases and the drift-flux model is used in the simulations. The reservoir has a geothermal temperature gradient and the overall heat transfer coefficient is 131.4 W/(m^2 °C). The bubble point pressure is here taken as constant (i.e., not a function of temperature) at $p_{bp} = 34.58$ MPa (5015 psia).

In this case the system is not at steady state. Rather, we consider primary production in which the reservoir pressure declines with time due to fluid withdrawal (the reservoir is sealed on all boundaries). Because p_1^w is held constant, this results in decreased liquid production with time. Simulation results are presented in Figs. 7–9. In Fig. 7, the pressure profile along the well is shown for $t = 1$ and 100 days. The fluid flow rates at standard conditions at $t = 1$ day are $q_o = 714.2$ m^3/day, $q_w = 1007$ m^3/day and $q_g = 1.462 \times 10^5$ m^3/day. At $t = 100$ days the flow rates are $q_o = 503.1$ m^3/day, $q_w = 649.8$ m^3/day and $q_g = 1.870 \times 10^5$ m^3/day. The decrease of pressure with time is clearly evident. The discontinuities in flow quantities are due to the well branching and segment numbering. At 1 day, the pressure in some segments is above the bubble point pressure (p_{bp} is shown as the horizontal dashed line in Fig. 7), while at 100 days the pressure is lower than the bubble point pressure everywhere along the well. This has an impact on the gas volume fraction, α_g, as shown in Fig. 8. Specifically, at 1 day, the gas phase is present only in segments 1–18 and 22–41. At 100 days, α_g is nonzero in all segments.

Along the horizontal branches α_g does not vary much. There is more variation along the vertical branch, where the pressure gradient is larger. Also, there is a jump in α_g at segment 11, where the upper horizontal branch meets the vertical branch. For example, at $t = 100$ days, this jump can be understood in terms of the gas phase flow rates in the two adjacent branches. More specifically, a smaller gas phase flow rate leaves segment 12 of the vertical branch (where $\alpha_g = 0.124$) and mixes with the larger gas phase flow leaving segment 22 of the horizontal branch (where $\alpha_g = 0.262$; this higher value of α_g is due to the lower pressure in the upper horizontal branch). This results in $\alpha_g = 0.172$ in segment 11.

The temperature profiles at 1 day and 100 days are shown in Fig. 9. The general appearance of the profiles is the same at both times, though there is a shift toward lower temperatures as time proceeds. The temperature is seen to consistently decrease in the direction of flow along both horizontal branches. This is due to the interplay of the Joule-Thompson effect and heat loss to the reservoir.

In our final example we consider a two-phase (gas and water) system with a vertical well 304.8 m in length and 0.0762 m in diameter. The well contains 21 segments, has only one perforation (at $z = L$), and is specified to produce liquid water at a rate of 159.0 m^3/day. No components other than water are present in this example. The initial reservoir pressure at $z = L$ is 15.16 MPa (2200 psi). As in the previous example, the reservoir pressure decreases with time due to fluid withdrawal. The bubble point occurs at a pressure of 6.89 MPa (1000 psi) at a temperature of 285 °C. The overall heat-transfer coefficient is $U_{to} = 105.2$ W/(m^2 °C).

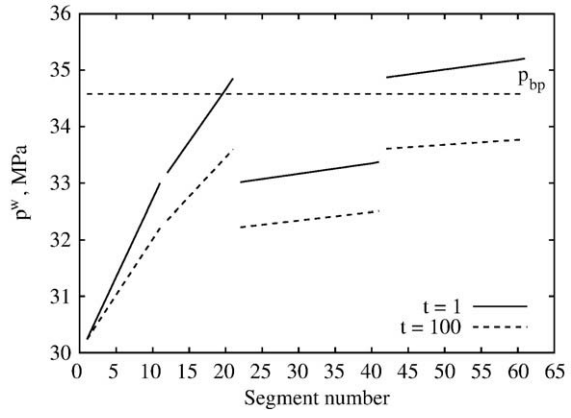

Fig. 7. Pressure variation at $t = 1$ and 100 days for the multilateral well example.

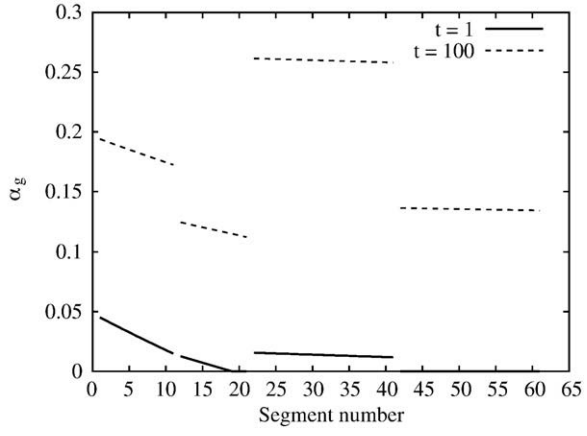

Fig. 8. Gas volume fraction at $t = 1$ and 100 days for the multilateral well example.

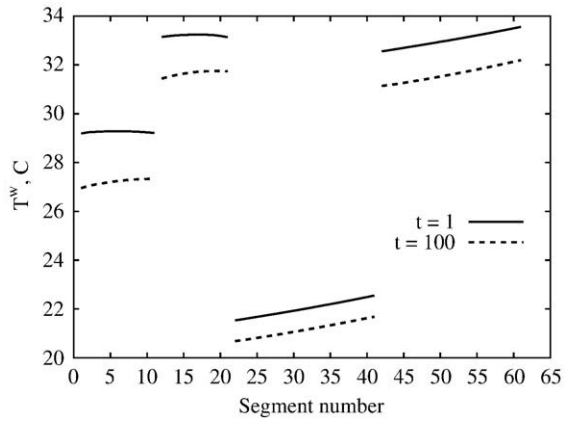

Fig. 9. Temperature variation at $t=1$ and 100 days for the multilateral well example.

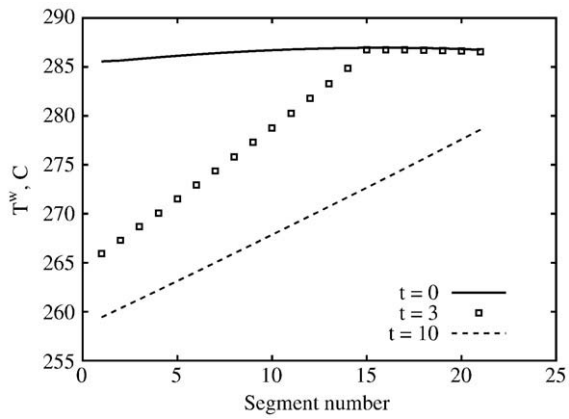

Fig. 11. Temperature variation at $t=0$, 3 and 10 days for the water production case.

Simulation results for the gas (water vapor) phase volume fraction along the well are shown in Fig. 10. Results for the temperature profile are presented in Fig. 11. At $t=3$ days, hot water enters the well at segment 21. Due to heat losses to the reservoir and decreasing pressure, this fluid reaches the bubble point pressure at segment 14. From this point to the first segment the gas phase is also present. In this two-phase region temperature is a function of pressure ($p^w = p^w_{sat}(T^w)$) and can be interpolated from steam tables (Keenan et al., 1969) as described earlier. At later times (e.g., $t=10$ days), due to the decrease in reservoir pressure, the fluid entering the well is already below the bubble point, so both phases exist along the well. As time proceeds and α_g increases, the total amount of fluid (gas + liquid) produced increases because a constant liquid rate (159.0 m^3/day) is maintained. Specifically, at a time of 3 days, $q_g = 1.312\times10^4$ m^3/day, and at a time of 10 days, $q_g = 1.803\times10^4$ m^3/day.

We now comment briefly on the computational requirements of the numerical thermal multiphase wellbore flow model. Here we report the average number of Newton iterations per time step required by the model and compare this to the requirements for the isothermal case. For the multilateral well example presented above, our model required an average of 7 or 8 Newton iterations per time step (depending on the maximum time step, which we varied from 0.1 days to 10 days). If we simulate this model without including energy effects (i.e., we solve the wellbore and reservoir flow equations but not the energy equations), the average number of Newton iterations per time step varies from about 4 to 6. Thus, as a result of the additional nonlinearity introduced by thermal effects, more Newton iterations are required for the coupled thermal problem. Similar numbers of Newton iterations per time step were required for other complex examples such as those presented in (Livescu et al., 2008a).

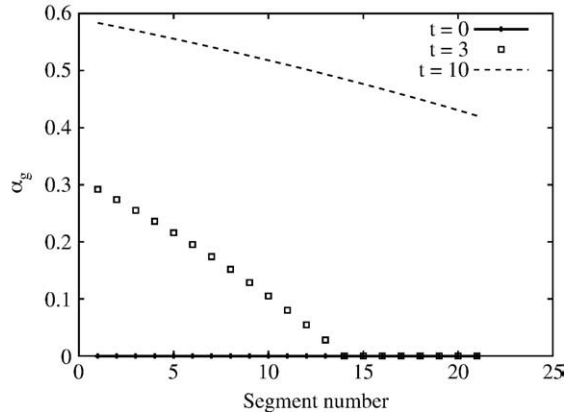

Fig. 10. Gas (water vapor) volume fraction variation at $t=0$, 3 and 10 days for the water production case.

The examples presented in this section demonstrate the wide variety of problems that can be addressed with our thermal wellbore flow model. The model allows for the simulation of general multilateral wells, three flowing phases, phase change, and full interaction between the well and the reservoir. The validation and verification examples are very encouraging as they suggest that the model is capturing the correct physics and that the numerical implementation properly represents the underlying formulation.

5. Concluding remarks

In this work, a numerical thermal multiphase wellbore flow model was developed and tested. This model is coupled with a general purpose reservoir simulator, so the combined formulation allows us to simulate many practical and important flow phenomena. The model entails the spatial (axial) and temporal discretization of the well domain and solution of discrete wellbore equations for mass conservation (for oil, water and gas components), energy conservation, and a pressure drop relationship. The slip between phases is represented using a drift-flux model. Heat loss to the surroundings is captured using an overall heat transfer coefficient. The model is solved fully-coupled with the reservoir flow equations.

We presented a series of numerical results, including validation against experimental results from Hasan and Kabir (2002) for a vertical well, verification against an analytical solution for three-phase steady-state flow, simulation of thermal multiphase flow in a multilateral well, and phase change (vaporization of water to steam) in a vertical well. Taken in total, these results demonstrate the accuracy and broad applicability of this model.

Acknowledgments

We are grateful to Shell Oil Company for providing funding for this work. We thank Huanquan Pan, Denis Voskov and Hamdi Tchelepi for many useful discussions and suggestions.

References

Aziz, K., Settari, A., 2002. Petroleum reservoir simulation. Blitzprint Ltd., Calgary.
Aziz, K. and Wong, T.W. Considerations in the development of multipurpose reservoir simulation models, Proceedings of the 1st and the 2nd International Forum on Reservoir Simulation, Alpbach, Austria, Sept. 12-16, 1988 and Sept. 4-8, 1989.
Bonizzi, M., Issa, R.I., 2003. On the simulation of three-phase slug flow in nearly horizontal pipes using the multi-fluid model. Int J Multiphase Flow 29, 1719–1747.
Cao, H. Development of techniques for general purpose simulators, Ph.D. dissertation, Stanford University, 2002.
Cheng, L., Mewes, D., 2006. Review of two-phase flow and flow boiling of mixtures in small and mini channels. Int J Multiphase Flow 32, 183–207.

Farouq Ali, S.M. and Abou-Kassem, J. Simulation of thermal recovery processes, Proceedings at the 1st and the 2nd International forum on reservoir simulation, Alpbach, Austria, Sept. 12-16, 1988 and Sept. 4-8, 1989.
Govier, G.W., Aziz, K., 1972. The flow of complex mixtures in pipes. Van Nostrand Reinhold Co., New York. (reprinted with some updates by the Society of Petroleum Engineers, Richardson, TX, 2008).
Hasan, A.R., Kabir, C.S., 2002. Fluid flow and heat transfer in wellbores. Society of Petroleum Engineers, Richardson, TX.
Hasan, A.R., Kabir, C.S., Lin, D., 2005. Analytic wellbore-temperature model for transient gas-well testing, SPE Paper 84288. SPE Res Eval Eng 8 (3), 240–247 June.
Hibiki, T., Ishii, M., 2003. One-dimensional drift-flux model and constitutive equations for relative motion between phases in various two-phase flow regimes. Int J Heat Mass Transfer 46, 4935–4948.
Hoeld, A., 2007. Coolant channel module CCM — a universally applicable thermal-hydraulic drift-flux based mixture-fluid 1D model and code. Nuclear Eng Des 237, 1952–1967.
Holmes, J.A., Barkve, T., Lund, O., 1998. Application of a multisegment well model to simulate flow in advanced wells. SPE Paper 50646, presented at the European Petroleum Conference, The Hague, Netherlands, Oct. 20-22, 1998.
Ishii, M., Hibiki, T., 2006. Thermo-fluid dynamics of two-phase flow. Springer Inc., New York.
Ishii, M., Mishima, K., 1984. Two-fluid model and hydrodynamic constitutive relations. Nuclear Eng Des 82, 107–126.
Issa, R.I., Kempf, M.H.W., 2003. Simulation of slug flow in horizontal and nearly horizontal pipes with the two-fluid model. Int J Multiphase Flow 29, 69–95.
Izgec, B., Kabir, C.S., Zhou, D., Hasan, A.R., 2007. Transient fluid and heat flow modeling in coupled wellbore/reservoir systems, SPE Paper 102070. SPE Res Eval Eng 10 (3), 294–301 June.
Jiang, Y. A flexible computational framework for efficient integrated simulation of advanced wells and unstructured reservoir models, Ph.D. dissertation, Stanford University, 2007.
Keenan, J.H., Keyes, F.G., Hill, P.G., Moore, J.G., 1969. Steam Tables. John Wiley & Sons.
Livescu, S., Durlofsky, L.J., Aziz, K., Ginestra, J.-C., 2008a. Application of a new fully-coupled thermal multiphase wellbore flow model. SPE Paper 113215, presented at the SPE Improved Oil Recovery Symposium, Tulsa, OK, April 19-23, 2008.
Livescu, S., Durlofsky, L.J., Aziz, K., 2008b. A semianalytical thermal multiphase wellbore flow model for use in reservoir simulation. SPE Paper 115796, presented at the SPE Annual Technical Conference and Exhibition, Denver, CO, Sept. 21-24, 2008.
Livescu, S., Durlofsky, L.J., Aziz, K., 2009. Development and application of a fully-coupled thermal compositional wellbore flow model. SPE Paper 121306, presented at the SPE Western Regional Meeting, San Jose, CA, March 24-26, 2009.
Masella, J.M., Tran, Q.H., Ferre, D., Pauchon, C., 1998. Transient simulation of two-phase flows in pipes. Int J Multiphase Flow 24, 739–755.
Oddie, G., Shi, H., Durlofsky, L.J., Aziz, K., Pfeffer, B., Holmes, J.A., 2003. Experimental study of two and three phase flows in large diameter inclined pipes. Int J Multiphase Flow 29, 527–558.
Ouyang, L.B., Aziz, K., 2002. A mechanistic model for gas–liquid flow in horizontal wells with radial influx or outflux. Petrol Sci Tech 20, 191–222.
Peaceman, D.W., 1977. Fundamentals of Numerical Reservoir Simulation. Elsevier Scientific Pub. Co.
Pourafshary, P., Varavei, A., Sepehrnoori, K., Podio, A.L., 2009. A compositional wellbore/reservoir simulator to model multiphase flow and temperature distribution. J Pet Sci Eng 69 (1–2), 40–52 Nov.
Prats, M., 1982. Thermal recovery. SPE Monograph 7.
Ramey Jr., H.J., 1962. Wellbore heat transmission, SPE Paper 96. Trans Soc Petrol Eng AIME 225 (4), 427–435.
Satter, A., 1965. Heat losses during flow of steam down a wellbore, SPE Paper 1071. J Pet Tech 17 (7), 845.
Sharma, Y., Shoham, O., Brill, J.P., 1989. Simulation of downhole heater phenomena in production of wellbore fluids, SPE Paper 16904. SPE Prod Eng 4 (3), 309–312 Aug.
Shi, H., Holmes, J.A., Durlofsky, L.J., Aziz, K., Diaz, L.R., Alkaya, B., Oddie, G., 2005. Drift-flux modeling of two-phase flow in wellbores, SPE Paper 84228. SPE J 10 (1), 24–33 March.
Shi, H., Holmes, J.A., Diaz, L.R., Durlofsky, L.J., Aziz, K., June 2005. Drift-flux parameters for three-phase steady-state flow in wellbores, SPE Paper 89836. SPE J 10 (2), 130–137.
Stanislav, J.F., Koral, S., Nicholson, M.K., 1986. Intermitent gas–liquid flow in upward inclined pipes. Int J Multiphase Flow 12, 325–335.
Stone, T.W., Edmunds, N.R., Kristoff, B.J., 1989. A comprehensive wellbore/reservoir simulator. SPE Paper 18419, presented at the SPE Symposium on Reservoir Simulation, Houston, TX, Feb. 6-8, 1989.
Stone, T.W., Bennett, J., Law, D.H.-S., Holmes, J.A., 2002. Thermal simulation with multisegment wells, SPE Paper 78131. SPE Res Eval Eng 5 (3), 206–218 June.
U.S. Department of Energy, Office of Naval Petroleum and Oil Shale Reserves, Strategic Significance of America's Oil Shale Resources, DOE Report, March 2004.
U.S. Department of Energy, Office of Petroleum Reserves, Office of Naval Petroleum and Oil Shale Reserves, Secure Fuels from Domestic Resources, DOE Report, June 2007.
Zuber, N., Findlay, J.A., 1965. Average volumetric concentration in 2-phase flow systems. J Heat Transfer 87 (4), 453.